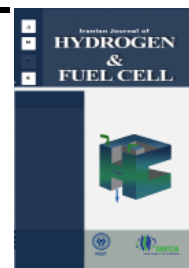


Iranian Journal of Hydrogen & Fuel Cell

**IJHFC**

Journal homepage://ijhfc.iroست.ir



## **Influence of unsuitable operational conditions on the transient performance of a small hydrogen liquefier**

**Ali Saberimoghaddam\* , Mohammad Mahdi Bahri Rasht Abadi**

Department of Chemistry and Chemical Engineering, Faculty of Chemical Engineering,  
Malek Ashtar University of Technology (MUT), Lavizan, Tehran, Iran

### **Article Information**

Article History:

Received:

02 Oct 2016

Received in revised form:

09 Dec 2016

Accepted:

15 Jan 2017

### **Keywords**

Heat exchanger

Joule-Thomson

Transient

Hydrogen

Refrigeration

### **Abstract**

Joule-Thomson cooling systems are used in refrigeration processes such as cryogenic gas liquefaction. Although extensive studies have been carried out by researchers, most studies include cryogenic heat exchangers and their associated fields. In the current study, an attempt was made to indicate the effect of using inappropriate operational conditions in a cryogenic Joule-Thomson cooling system including a recuperative heat exchanger, expansion valve, and collector. Mass flow rate and operational pressure were selected as design parameters while cool-down time and final temperature of high-pressure gas at heat exchanger outlet were considered as responses. The results showed that using a mass flow rate smaller than the design value led to considerable decrease in performance. Operational pressure had less effect on cool-down time. Increasing the pressure had no significant effect on the gas temperature at the expansion valve inlet for high mass flow rates. Using unsuitable values for the mass flow rate and operational pressure might lead to failed liquefaction despite using a heat exchanger with high effectiveness.

## **1. Introduction**

According to a report published by the Intergovernmental Panel on Climate Change (IPCC), the world needs to focus on continuing the development of clean technologies and energy storage systems to address global climate change

[1]. Hydrogen is a clean-burning fuel, and when combined with oxygen in a fuel cell it produces heat and electricity with only water vapor as a by-product [2]. But hydrogen does not exist freely in nature. It is only produced from other sources of energy and is often referred to as an energy carrier, that is, an efficient way to store and transport energy. Hydrogen

is currently produced from several methods such as steam methane reforming or electrolysis. Storing energy in the form of hydrogen could help address the growing problems facing this world related to our growing energy consumption.

There are various methods of storing hydrogen including compression, metal hydrides, storage as a cryogenic liquid or a combination of these. Storage of hydrogen as a liquid offers a low pressure high energy density fuel that can be used in a variety of applications. In the past, liquid hydrogen (LH<sub>2</sub>) was widely known for its use as a rocket fuel. Today, there are many applications for this high energy density fuel such as the development of fuel cell vehicles using cryo-compressed hydrogen storage tanks by Lawrence Livermore National Laboratory, BMW, and Linde Group. Small size hydrogen liquefiers are easy to operate and are mainly built to serve as a test facility to produce liquid hydrogen on demand. Liquefied hydrogen is used in the aerospace and electronics industry, and in the future it may be used as a fuel for public transportation. In economically flourishing countries there is an increasing demand for hydrogen at rocket test sites, whereas in high tech industry ultra pure hydrogen is needed.

For small hydrogen liquefiers there is a sharp decrease in energy requirements if the liquefaction capacity is increased, whereas for larger plants there is no significant difference. For this reason, designing a smaller hydrogen liquefier considering maximum hydrogen liquefaction could decrease energy consumption needed for small size hydrogen liquefier to operate. To increase the hydrogen liquefaction percentage in small hydrogen liquefiers, suitable operational conditions must be considered for a Joule-Thomson cooling system [3, 4]. Joule-Thomson cooling systems are used in the refrigeration and gas liquefaction processes. Simple design, no moving parts, high reliability, less maintenance, and low cost are the main benefits of gas liquefiers operating with Joule-Thomson methods [5, 6].

The most important element of such gas liquefiers is the counter current recuperative heat exchanger operating at cryogenic temperatures. Pacio and

Dorao [7] reviewed the thermal hydraulic models of cryogenic heat exchangers. They introduced physical effects such as changes in fluid properties, flow maldistribution, axial longitudinal heat conduction, and heat leakage as the main challenges of cryogenic heat exchangers. Aminuddin and Zubair [8] studied the various losses in a cryogenic counter flow heat exchanger numerically. They discussed the effect of longitudinal heat conduction loss as parasitic heat loss by conduction from the heat exchanger cold end to the adjacent components, but they did not perform any experimental tests.

Krishna et al. [9] studied the effect of longitudinal heat conduction in the separating walls on the performance of a three-fluid cryogenic heat exchanger with three thermal communications. They reasoned that the thermal performance of heat exchangers operating at cryogenic temperature is strongly governed by various losses such as longitudinal heat conduction through the wall, heat in-leak from the surroundings, flow maldistribution, etc. Gupta et al. [10] investigated the second law analysis of counter flow cryogenic heat exchangers in the presence of ambient heat in-leak and longitudinal heat conduction through the wall. They cited the importance of considering the effect of longitudinal heat conduction in the design of cryogenic heat exchangers.

Nellis [11] presented a numerical model of the heat exchanger in which the effect of axial conduction, property variations, and parasitic heat losses to the environment have been explicitly modeled. He concluded that small degradation exists in the performance of the heat exchanger at conditions where the temperature of the heat exchanger cold end is equal to the temperature of the inlet cold fluid. Narayanan and Venkatarathnam [12] presented a relationship for the effectiveness of a heat exchanger losing heat at the cold end. They studied a Joule-Thomson cryo-cooler and concluded that the hot fluid outlet temperature will be lower in the heat exchangers with heat in-leak at the cold end with respect to heat exchangers with insulated ends. Ranganayakulu et al. [13] studied the effect of longitudinal heat conduction in a compact plate

fin and tube fin heat exchanger using the finite element method. They indicated that the thermal performance deteriorations of cross flow plate-fin, cross flow tube-fin and counter flow plate-fin heat exchangers due to longitudinal heat conduction may become significant, especially when the fluid capacity rate ratio is equal to one and when the longitudinal heat conduction parameter is large.

Damle and Atrey [5] studied the effect of reservoir pressure and volume on the cool-down behavior of a miniature Joule-Thomson cryo-cooler considering the distributed Joule-Thomson effect in the heat exchanger tube. Chou et al. [14] presented a preliminary experimental and numerical study of transient characteristics for a miniature Joule-Thomson cryo-cooler. Tzabar and Kaplansky [15] analyzed the cool-down process for Dewar-detector assemblies cooled with Joule-Thomson cryo-coolers by the finite element method. Hong et al. [16] studied the cool-down characteristics of a miniature Joule-Thomson refrigerator. They discussed the influence of the supply pressure and the temperature on the mass flow rate during the cool-down stage. Maytal [17] studied the cool-down periods of a fast Joule-Thomson cryo-cooler for nitrogen and argon as coolants. Chien et al. [18] performed an experimental and numerical study of transient characteristics for the self-regulating Joule-Thomson cryo-cooler. They developed modeling of the bellows control mechanism and the simulation of the cooler system. These studies commonly consist of Joule-Thomson cryo-coolers with Hampson type heat exchangers. Moreover, most of them include a laboratory scale unit and do not studied the operational parameters.

A simple Joule-Thomson cooling system includes a recuperative heat exchanger, expansion valve, and collector/evaporator. The collector is used in the gas the gas liquefaction process to collect liquefied gas while the evaporator is used for refrigeration purposes. Several parameters, such as operational pressure, mass flow rate, pre-cooling temperature, etc., determine the performance of Joule-Thomson cooling systems. Some of these have a negative influence while others have a positive influence

on Joule-Thomson cooling systems. Therefore, selecting suitable operational conditions is difficult and there is no straightforward method to estimate optimum parameters. In the case of cryogenic processes, the time needed for the cool-down process and power consumption are the main challenges. Sometimes an operational run may take as long as one day. In addition, investigating some parameters may be difficult due to special conditions such as very low temperatures or high pressures needed for common cryogenic operations.

Any change in operational conditions may result in decreasing performance and efficiency. A gas liquefier must operate in designed conditions. Using mass flow rates lower than the designed value leads to a decrease in performance and efficiency. On the other hand, using operational pressure lower/higher than the designed value may influence the system performance. Heat exchangers are mechanically designed based on the minimum allowable pressure drop inside the tubes and an optimum heat transfer surface area. Commonly, heat exchangers are studied individually without considering joined devices such as the expansion valve and collector. When a heat exchanger is used in a Joule-Thomson cooling system its thermal behavior is dependent on joined devices. In this condition the heat exchanger, expansion valve, and collector must be considered simultaneously. In the present work, an attempt was made to evaluate the performance of a small hydrogen liquefier (as a case study of a Joule-Thomson cooling system) operating in the conditions different from designed values. Mass flow rate and operational pressure were selected as independent variables while cool-down time and upstream temperature of expansion valve were selected as dependent answers.

---

## 2. Problem description

Fig. 1 shows the recuperative tube in the tube heat exchanger in which the high pressure gas flows inside the inner tube and the low pressure gas returns through annulus. The high pressure gas exchanges

energy with the low pressure gas and passes through the expansion valve. The high pressure gas temperature drops down due to Joule-Thomson expansion. The cooled low pressure gas returns from the annulus and cools the incoming high pressure gas. As time proceeds, the high pressure gas temperature at the heat exchanger outlet gradually decreases. This process continues until the high pressure gas partially transforms into liquid at the expansion valve outlet. The high pressure gas temperature at the heat exchanger outlet (upstream of the expansion valve) determines the liquid fraction of gas at the expansion valve outlet. A recuperative heat exchanger can decrease the high pressure gas temperature to a specified value based on the operational pressure and heat transfer coefficient inside the tubes.

Since a heat exchanger is designed based on the operational pressure and mass flow rate, using an operational pressure and mass flow rate different from the designed values can change the heat transfer coefficient and heat exchanger performance. This phenomenon may increase cool-down time and decrease the liquid fraction at the expansion valve outlet. Unlike previously performed experimental works in which the results obtained from experimental tests have been directly used to study the problem, here the experimental data were used for validating the mathematical simulations and the results obtained from simulations were used to obtain a straightforward equation for investigating the transient behavior of the system. This procedure was used to eliminate the required time for performing

the experimental tests and considerable costs (the cost for preparing high pressure hydrogen and liquid nitrogen) needed to reach from start time to steady state conditions.

Two operational tests were performed by a Joule-Thomson cooling system operating in a gas liquefier. The first was performed to obtain the effective mass of the collector and modify the correlations of convection heat transfer coefficient for gas streams inside the heat exchanger. This test was carried out using nitrogen gas as the working fluid. The second test was performed to validate the mathematical model using helium gas and operational conditions. After the validation step, a surface fitting method was used and a unique polynomial equation was obtained for each answer. The main subject of the current study is to evaluate the performance of a Joule-Thomson cooling system operating in conditions different from the designed specified conditions for hydrogen liquefaction.

### 3. Experimental test procedure

Experimental tests were performed using a small gas liquefier. Nitrogen and helium gas were used as working fluids. Pre-cooling was performed using a coiled tube immersed in a liquid nitrogen bath. In order to avoid liquefying high-pressure nitrogen gas within the bath, the liquid nitrogen level was adjusted at special level. The helically coiled tube in the tube heat exchanger, made from stainless steel 304 L, and the

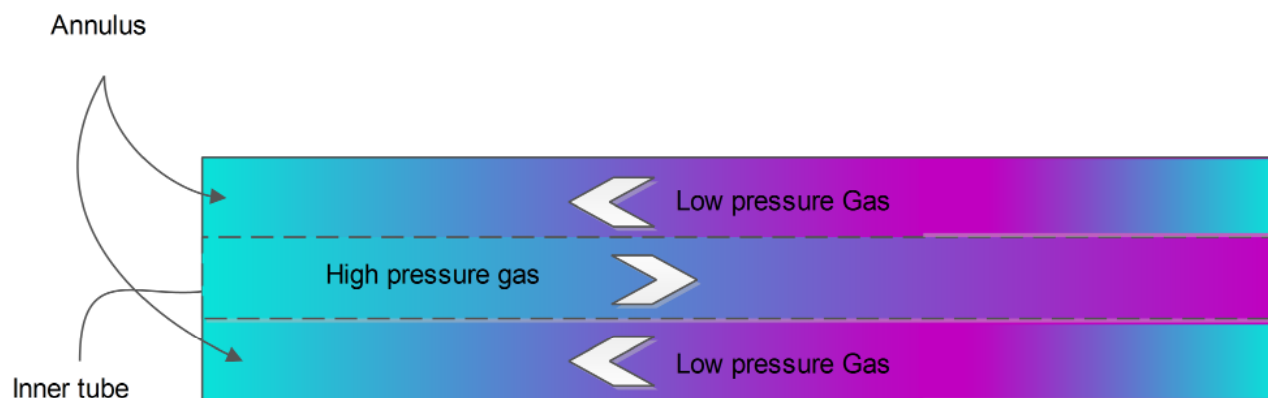


Fig. 1. Streams configuration within the recuperative tube in tube heat exchanger.

expansion valve were placed in a cold-box equipped with an evacuated jacket ( $10^{-9}$  bar). The details of the experimental Joule-Thomson cooling system are presented in Table 1.

**Table 1. The details of the experimental Joule-Thomson cooling system**

Parameters	Values
Inner tube internal diameter (mm)	1.671
Outer tube internal diameter (mm)	8.001
Tubes wall thickness (mm)	0.762
Tube length (m)	4
Tube wall thermal conductivity ( $\text{W m}^{-1} \text{K}^{-1}$ )	50

The vacuum conditions within the cold-box were established using a Woosung rotary vacuum pump ( $5 \text{ m}^3 \text{ h}^{-1}$ ) and a DP-100 diffusion vacuum pump ( $250 \text{ l s}^{-1}$ ) in series. Temperatures were measured by Pt-100 sensors installed on the tube wall with an accuracy of 0.1 K. The details of how the cryogenic temperature was measured have been reported by Saberimoghaddam and Bahri Rasht Abadi [6]. The gas pressure was measured at several points in the recuperative heat exchanger; including the inlet of high pressure side, outlet of high pressure side (upstream of expansion valve), inlet of low pressure side (downstream of expansion valve), and outlet of low pressure side. The value of pressure drop along the heat exchanger tubes was negligible during the experimental tests. The volumetric flow was measured by a rotameter flow meter calibrated for nitrogen and helium gas. The rotameter was installed downstream of the expansion valve. Inset paragraph After measuring the volumetric flow rate using the Peng-Robinson equation of state in Aspen Hysys software and considering given conditions (ambient temperature and atmospheric pressure) the volumetric flow rates were converted to mass flow rates. Fig. 2 shows the process flow diagram of the gas liquefier. As can be seen, the Joule-Thomson cooling system has been specified by a bold line. The pressurized gas is pre-cooled in two heat exchangers (initial heat exchanger and liquid nitrogen bath). After pre-cooling, the gas enters the Joule-Thomson

cooling section. It must be noted that in our small hydrogen liquefier, the compressor indicated in Fig. 2 was substituted with a high pressure gas cylinder due to technical limitations.

## 4. Modeling procedure

Finite Element Method (FEM) was used to solve the energy equations in the counter current helically coiled tube in the tube heat exchanger. Forward, central, and backward forms of FEM were used to discretize the energy equations in the warm fluid, tubes wall, and cold fluid, respectively. MATLAB m-file programming was employed to solve the FEM forms of energy equations using the Gauss–Jordan method. The properties of gas at various temperatures were collected from Aspen Properties software version 7.1 and added to a separate function m-file of MATLAB software. This function m-file was used in the main code. The assumptions applied to simulate the problem were as follows:

- The radial distribution of temperature was neglected in gas flows and tubes wall.
- Conduction and convection heat in-leak terms were neglected (high vacuum conditions).
- Pressure drops along the tubes were measured in the gas liquefier and set to zero in the simulation.
- In equation (5), the low-pressure gas temperature at the collector outlet was set to the collector temperature.

The model was solved by direct use of heat capacities, radiation heat transfer into the outer tube wall, and longitudinal heat conduction through separating and external walls. The energy equations were established in five sections (warm fluid, cold fluid, separating wall, external wall, and collector) as follows:

$$\rho_1 A_1 c_{p1} \frac{dT_1}{dt} = -m_1 c_{p1} \frac{dT_1}{dz} - h_1 (2\pi r_1) (T_1 - T_2) \quad (1)$$

$$\rho_2 A_2 c_{p2} \frac{dT_2}{dt} = k_2 A_2 \frac{d^2 T_2}{dz^2} + h_1 (2\pi r_1) (T_1 - T_2) - h_3 (2\pi r_2) (T_2 - T_3) \quad (2)$$

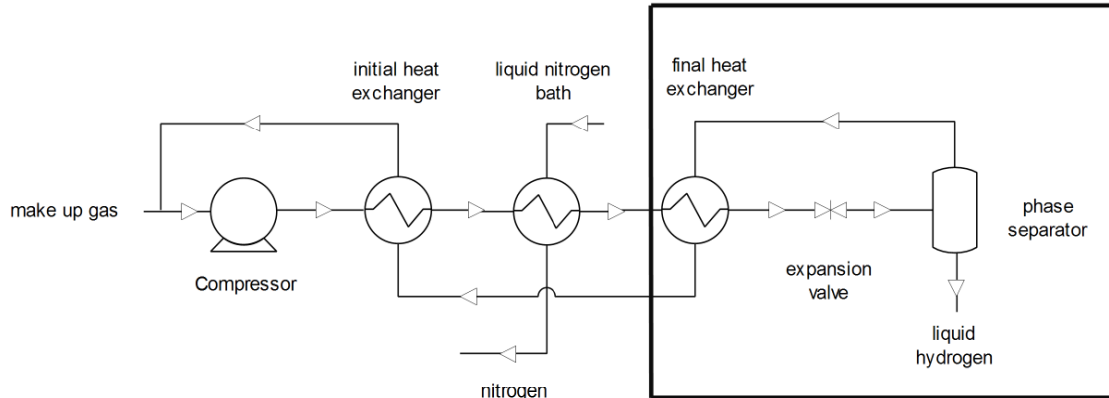


**Fig. 2. Process flow diagram of a small gas liquefier. The bold line specifies the Joule-Thomson cooling system including the recuperative heat exchanger, expansion valve, and collector.**

$$\rho_3 A_3 c_{p3} \frac{dT_3}{dt} = m_3 c_{p3} \frac{dT_3}{dz} + h_3 (2\pi r_2) (T_2 - T_3) + h_3 (2\pi r_3) (T_4 - T_3) \quad (3)$$

$$T_3(z=l) = f[T_1(z=l)]$$

$$T_4(z=0) = T_{Pre-cooling} \text{ and } T_4(z=l) = f[T_1(z=l)]$$

$$\rho_4 A_4 c_{p4} \frac{dT_4}{dt} = k_4 A_4 \frac{d^2 T_4}{dz^2} - h_3 (2\pi r_3) (T_4 - T_3) + Q_i (2\pi r_4) \quad (4)$$

$$m_c c_{pc} \frac{dT_c}{dt} = m_1 c_{p3} T_{J-T} - m_3 c_{p3} T_c \quad (5)$$

Where the subscript "c" indicates the collector properties. The value of  $T_{J-T}$  was calculated as follows:

$$T_{J-T} = f[T_1(z=l)] \quad (6)$$

Where  $f[T_1(z=l)]$  is a function of the warm gas outlet temperature (upstream of the expansion valve) to apply the Joule-Thomson effect in calculations. The term  $f[T_1(z=l)]$  was coded using a separate function m-file and used in the main program. The  $Q_i$  was defined as a heat in-leak term by a radiation heat transfer mechanism as follows:

$$Q_i = \epsilon \sigma (T_a^4 - T_4^4) \quad (7)$$

The boundary conditions are as follows:

$$T_1(z=0) = T_{Pre-cooling}$$

$$T_2(z=0) = T_{Pre-cooling} \text{ and } T_2(z=l) = f[T_1(z=l)]$$

A simple geometry of the heat exchanger and streams configuration is shown in Fig. 3.

In order to estimate the convection heat transfer coefficient within the helically coiled tube, the correlations proposed by Xin and Ebadian were used as follows [19]:

$$Nu_{ave} = (2.153 + 0.318 De^{0.643}) Pr^{0.177} \quad (8)$$

$$20 < De < 2000, 0.7 < Pr < 175,$$

$$0.0267 < \frac{d}{D_{coil}} < 0.0884$$

$$Nu_{ave} = 0.00619 Re^{0.92} Pr^{0.4} \left( 1 + \frac{3.455d}{D_{coil}} \right) \quad (9)$$

$$5 \times 10^3 < Re < 10^5, 0.7 < Pr < 5,$$

$$0.0267 < \frac{d}{D_{coil}} < 0.0884$$

Equations (8) and (9) were used in high-pressure and low-pressure gas, respectively. The program was able to select the appropriate equation for the flows according to the flow regime during the computational run. After performing the first experimental test (with nitrogen gas), equations (8) and (9) were modified by a 30% decrease in the final value of the convection heat transfer coefficient. The modified equations had good agreement with the second experimental test using helium gas. The modified equations were used

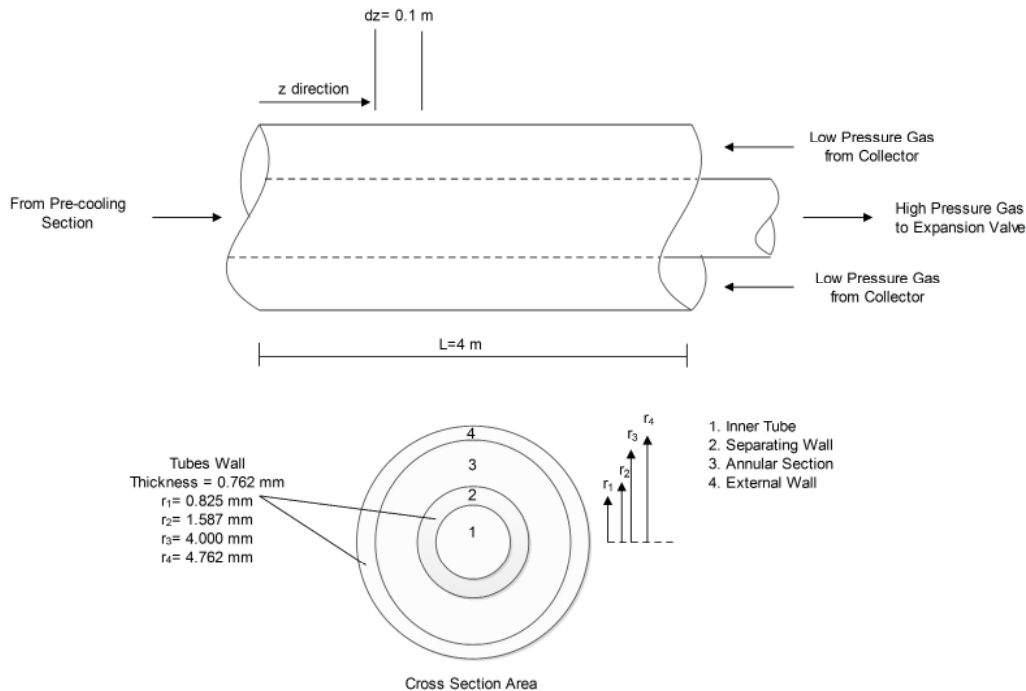


**Fig. 3. Scheme of recuperative heat exchanger and streams configuration. The heat exchanger is a helically coiled tube in the tube equipment but it has been drawn as straight tubes to simply show the geometry. in the simulations for hydrogen gas.**

## 5. Model Validation

Validating the model was carried out in two steps. The first step used nitrogen gas as the working fluid to determine the effective mass of the collector engaged in the cool-down process and convection heat transfer coefficients. The collector is used to collect the liquefied gas. According to our preliminary experimental tests, the cool-down rate of the collector at different points was not the same. Therefore, an effective mass with the same temperature throughout the collector was assumed for the system and used in the simulation. The model with an assumption of  $0.1\text{ kg}$  effective mass of the collector predicted the first experimental test results with a good agreement. Fig. 4 shows the results obtained from the experimental test and simulation. In the simulation, the heat exchanger inlet temperatures obtained from the experiment were used as boundary conditions in the mathematical model. As can be seen, the heat exchanger outlet temperatures have been predicted by the mathematical model with  $5\%$  relative error.

Due to complicated geometry and the assumption of an effective mass for the collector, this relative error is acceptable. Moreover, at  $40\text{ min}$ , a fluctuation occurred in the heat exchanger inlet temperature and its effects appeared in the heat exchanger outlet temperature. Influence of this fluctuation on heat exchanger outlet temperature can be observed in the simulation results. This means that the model is able to simulate the qualitative transient behavior of gas inside the heat exchanger tubes as well as temperature values. Fig. 5 shows the comparison between results obtained from the experiment and simulation using helium gas as the working fluid. Helium with a negative Joule-Thomson coefficient at ambient temperature and low density has maximum similarity with hydrogen gas. Therefore, helium gas was used in the second step of validation while the effective mass of collector and modified convection heat transfer coefficient obtained from first step was used in the model. As can be seen, the results obtained from the simulation have good agreement with experimental data, and the model can be used to analyze the transient behavior of any cryogenic gases.

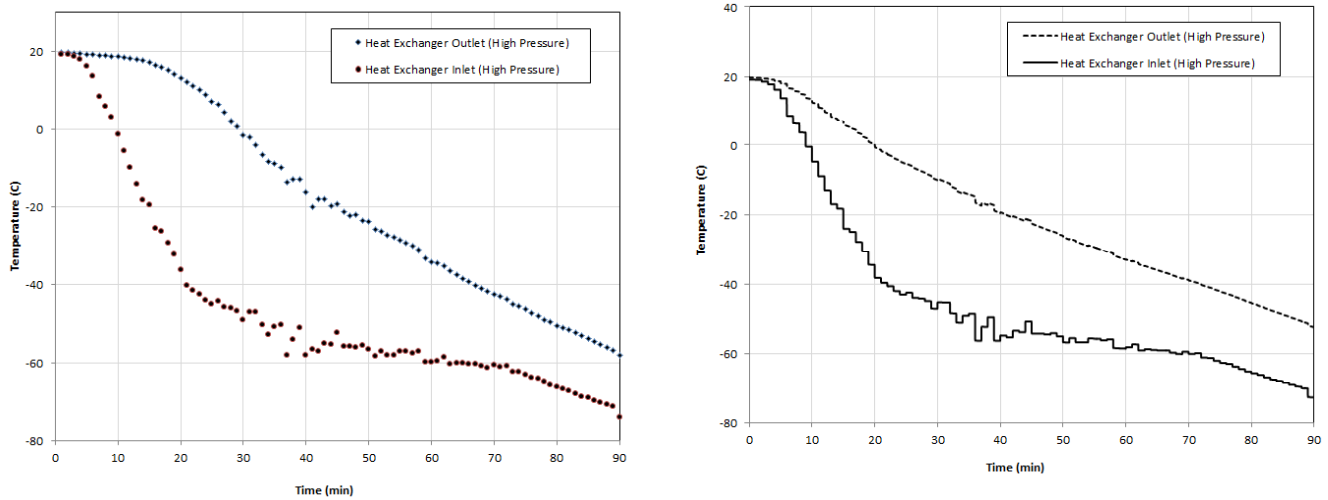


Fig. 4. Comparison between results obtained from the experimental test (left) and the simulation (right) for nitrogen gas.

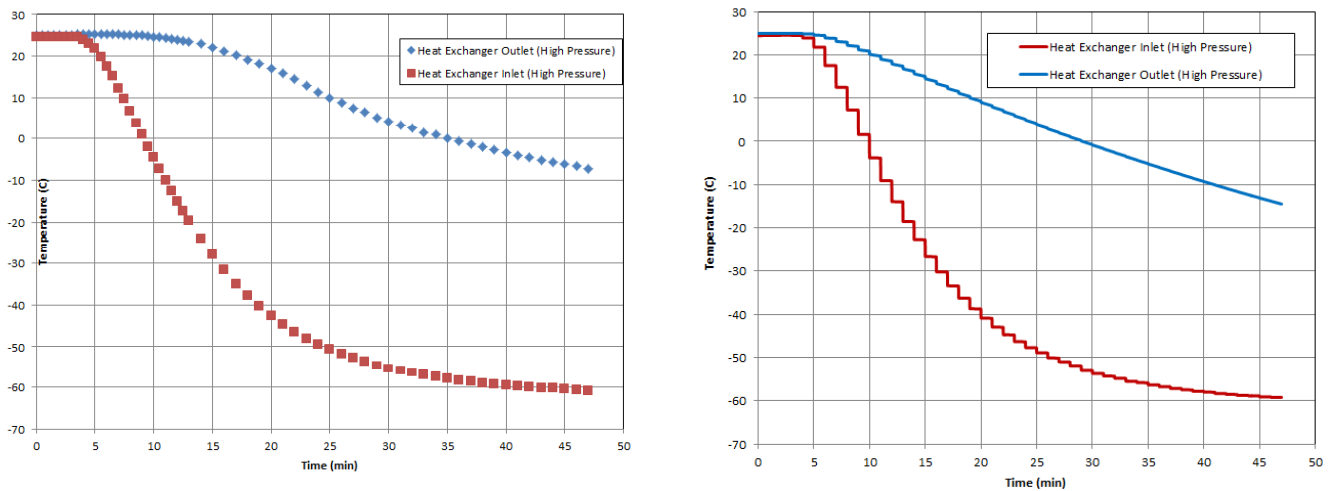


Fig. 5. Comparison between results obtained from the experimental test (left) and simulation (right) for helium gas.

## 6. Results and discussions

The small hydrogen liquefier has been designed for producing 500 cc/hr liquid hydrogen. Considering 16% liquefaction at the expansion valve outlet, the mass flow rate of hydrogen gas at the feed inlet must be 0.25 kg/hr at pressure equal to 80 bar.

In order to analyze the performance of a small Joule-Thomson gas liquefier in unsteady state conditions, several parameters were considered using a mathematical model for hydrogen as the working fluid. Operational pressure and mass flow rate are effective variables to determine efficiency and performance of the system. As mentioned above, the small hydrogen liquefier considered in the current research has been designed for a mass flow

rate and operational pressure equal to 0.25 kg h<sup>-1</sup> and 80 bar, respectively. The influence of using different operational conditions will be considered using a mathematical method. Several computational runs were performed with different mass flow rates and operational pressures. The results obtained from the computational runs are presented in Tables 2 to 5. Mass flow rate directly determines the convection heat transfer coefficients inside the heat exchanger tubes. In addition, the gas temperature at the expansion valve inlet and operational pressure determine the gas temperature at the expansion valve outlet based on the Joule-Thomson coefficient. The mentioned parameters are not independent. Different mass flow rates lead to obtain different temperatures at the expansion valve inlet and different cool-down times



**Table 2. Influence of mass flow rate on the cool-down time and performance of the small hydrogen liquefier (operational pressure of 60 bar and pre-cooling temperature of -196 °C)**

Mass flow rate (kg h <sup>-1</sup> )	Gas temperature at expansion valve inlet (°C)	Gas temperature at expansion valve outlet (°C)	Cool-down time (min)
0.05	-165	-170.6	360
0.10	-195	-206.8	250
0.15	-212	-230.7	200
0.20	-224	-250.6	155
0.25	-225	-252.2	96

**Table 3. Influence of mass flow rate on the cool-down time and performance of the small hydrogen liquefier (operational pressure of 80 bar and pre-cooling temperature of -196 °C)**

Mass flow rate (kg h <sup>-1</sup> )	Gas temperature at expansion valve inlet (°C)	Gas temperature at expansion valve outlet (°C)	Cool-down time (min)
0.05	-168	-174.0	360
0.10	-207	-223.2	250
0.15	-224	-250.6	140
0.20	-225	-252.3	85
0.25	-225	-252.3	60

**Table 4. Influence of mass flow rate on the cool-down time and performance of the small hydrogen liquefier (operational pressure of 100 bar and pre-cooling temperature of -196 °C)**

Mass flow rate (kg h <sup>-1</sup> )	Gas temperature at expansion valve inlet (°C)	Gas temperature at expansion valve outlet (°C)	Cool-down time (min)
0.05	-177	-187.6	360
0.10	-214	-238.7	250
0.15	-225	-252.3	150
0.20	-227	-252.3	90
0.25	-227	-252.3	60

**Table 5. Influence of mass flow rate on the cool-down time and performance of the small hydrogen liquefier (operational pressure of 120 bar and pre-cooling temperature of -196 °C)**

Mass flow rate (kg h <sup>-1</sup> )	Gas temperature at expansion valve inlet (°C)	Gas temperature at expansion valve outlet (°C)	Cool-down time (min)
0.05	-177	-188.4	360
0.10	-214	-239.2	250
0.15	-225	-252.3	150
0.20	-227	-252.3	90
0.25	-227	-252.3	60

at any pressure. Based on the Tables 2-5, pressure has less effect on the cool-down time than on the mass flow rate. Increasing the pressure leads to a decrease in gas temperature at the expansion valve inlet for lower mass flow rates. This phenomenon also takes place for higher mass flow rates, but gas with a higher mass flow rate partially transforms into liquid and this liquefied gas is collected in the collector. In this condition, the mass flow rate of the un-liquefied gas decreases and the gas returning from other side of the heat exchanger cannot decrease the incoming gas temperature lower than a specified value such as  $-225^{\circ}\text{C}$  or  $-227^{\circ}\text{C}$  due to lower heat capacity. For this reason, in steady state conditions, the high pressure gas temperature at the expansion valve inlet reaches a special value for any pair of mass flow rate and operational pressure. On the other side, for a given operational pressure, increasing the mass flow rate leads to a decrease in gas temperature at the expansion valve inlet, but this decrease is limited and further increase in mass flow rate cannot decrease the temperature and improve the liquefaction. For operational pressure equal to 60 bar, increasing the mass flow rate up to  $0.25\text{ kg h}^{-1}$  leads to a decrease in the gas temperature at the expansion valve inlet up to  $-225^{\circ}\text{C}$ . In the case of operational pressures equal to 80, 100, and 120 bar, the gas temperatures at

the expansion valve inlet reaches to  $-225$ ,  $-227$ , and  $-227^{\circ}\text{C}$ , respectively, for a mass flow rate equal to  $0.20\text{ kg h}^{-1}$ . Higher mass flow rate does not influence the gas temperature at the expansion valve inlet.

Fig. 6 shows the contour of temperature at the expansion valve inlet obtained from data presented in Tables 2-5. Dark blue areas (two temperature level areas) represent temperatures which can result in liquefaction at the expansion valve outlet. As can be seen, increasing the mass flow rate at constant pressure leads to a decrease in temperature at the expansion valve inlet. Increasing the pressure at mass flow rates higher than  $0.15\text{ kg h}^{-1}$  can result in liquefaction at the expansion valve outlet, but increasing the pressure at lower mass flow rates cannot liquefy the gas. The fitted polynomial equation obtained from MATLAB<sup>®</sup> surface fitting toolbox with R-square equal to 0.97 is as follows:

$$T = -99.83 - 0.3585 \times P - 1060 \times \dot{m} + 1.27 \times P \times \dot{m} + 2307 \times \dot{m}^2 \quad (10)$$

Where  $T$  is the temperature ( $^{\circ}\text{C}$ ),  $P$  is the pressure (bar), and  $\dot{m}$  is the mass flow rate ( $\text{kg h}^{-1}$ ). This equation is reliable for a pressure range of 60 - 120 bar and mass flow rates between 0.05 and  $0.25\text{ kg h}^{-1}$  for hydrogen gas. Differential change in temperature can be expressed as follows:

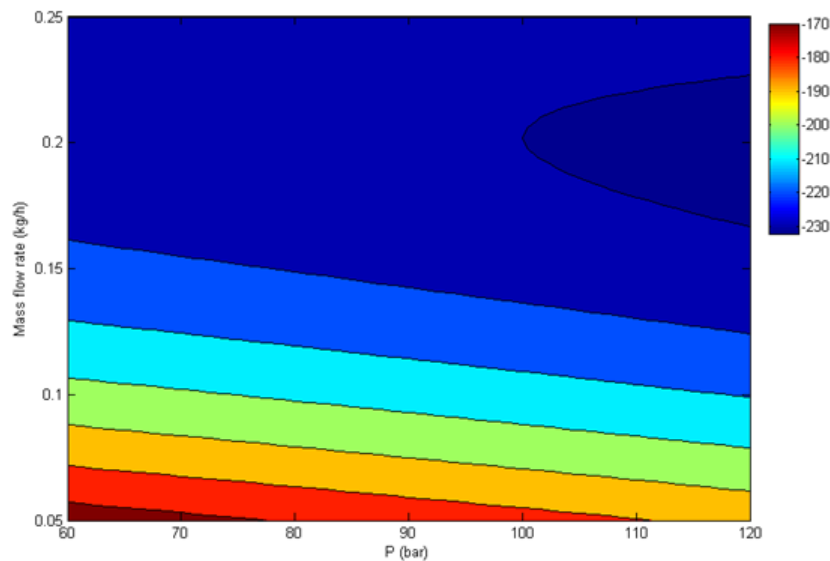


Figure 6. The contour of temperature at the expansion valve inlet obtained from data presented in Tables 1-4.

$$dT = (-0.3585 + 1.27 \times \dot{m}) dP + (-1060 + 1.27 \times P + 4614 \times \dot{m}) d\dot{m} \quad (11)$$

According to equation (11), assuming constant mass flow rate, the value of  $\frac{dT}{dP}$  will be a function of the mass flow rate and has a constant value. On the other word, the value of  $\frac{dT}{dP}$  will be lower (with negative value) at smaller mass flow rates. The value of  $\frac{dT}{dP}$  is -0.29 and -0.04 for mass flow rates of 0.05 and 0.25 kg h<sup>-1</sup>, respectively. This means that increasing the pressure has no significant effect on the gas temperature at the expansion valve inlet for high mass flow rates. When the mass flow rate is small, the convection heat transfer coefficient becomes low. Therefore, in order to compensate the defect of a lower convection heat transfer coefficient, the gas temperature must be lower at the expansion valve outlet. Increasing the pressure can increase the Joule-Thomson effect and consequently decrease the temperature level throughout the heat exchanger. Table 6 presents the convection heat transfer coefficient inside the inner tube and annulus. These values have been evaluated by Xin and Ebadian who suggested correlations for coiled tubes [19]:

$$Nu_{ave} = (2.153 + 0.318De^{0.643}) Pr^{0.177} \quad (8)$$

$$20 < De < 2000, 0.7 < Pr < 175,$$

$$0.0267 < \frac{d}{D_{coil}} < 0.0884$$

$$Nu_{ave} = 0.00619Re^{0.92} Pr^{0.4} \left( 1 + \frac{3.455d}{D_{coil}} \right) \quad (9)$$

$$5 \times 10^3 < Re < 10^5, 0.7 < Pr < 5,$$

$$0.0267 < \frac{d}{D_{coil}} < 0.0884$$

As can be seen, the convection heat transfer coefficients have maximum values for a mass flow rate of 0.25 kg h<sup>-1</sup> as the designed mass flow rate. A decrease in mass flow rate results in significant decrease in the convection heat transfer coefficient. This phenomenon takes place due to a decrease in superficial velocity of fluid inside the tube. Therefore, for a smaller mass flow rate, the diameter of the tube

must be decreased to increase the velocity of fluid. Since a change in the heat exchanger tube diameter is not possible after the manufacturing and installing step, using a designed value for the mass flow rate will be an important parameter to obtain optimum results. Fig. 7 shows the liquefaction percentage contours at various operational pressures and mass flow rates. As can be seen, decreasing the mass flow rate up to 0.12 kg h<sup>-1</sup> stops liquefaction. Fig. 7 confirms the above-mentioned discussion associated with the convection heat transfer coefficient. A decrease in the convection heat transfer coefficient has led to a decrease in the liquefaction of hydrogen.

Time and feed consumption are important parameters for a small hydrogen liquefier. Cool down time is considerable compared with the total operating time needed for producing one liter liquid hydrogen. Table 7, 8 and 9 present time and total mass of hydrogen required for producing one liter liquid hydrogen at 80 bar, 100 bar, and 120 bar, respectively. As can be seen, increasing the mass flow rate up to 0.25 kg h<sup>-1</sup> results in decreasing the time needed for producing one liter of liquid hydrogen. On the other hand, using mass flow rates smaller than 0.2 kg h<sup>-1</sup> leads to a considerable increase in the total mass of hydrogen, while using mass flow rates higher than 0.2 kg h<sup>-1</sup> has a negligible effect on the total mass of hydrogen. According to obtained results, it is suggested to use the designed mass flow rate at any operational pressure to decrease operational time, although the total mass of hydrogen will not considerably change.

## 7. Conclusion

In the current study, an attempt was made to indicate the effect of using inappropriate operational conditions in a cryogenic Joule-Thomson cooling system including a recuperative heat exchanger, expansion valve and collector. According to the discussion presented in previous sections, increasing the pressure with respect to an increase in mass flow rate, has less effect on cool-down time. Increasing

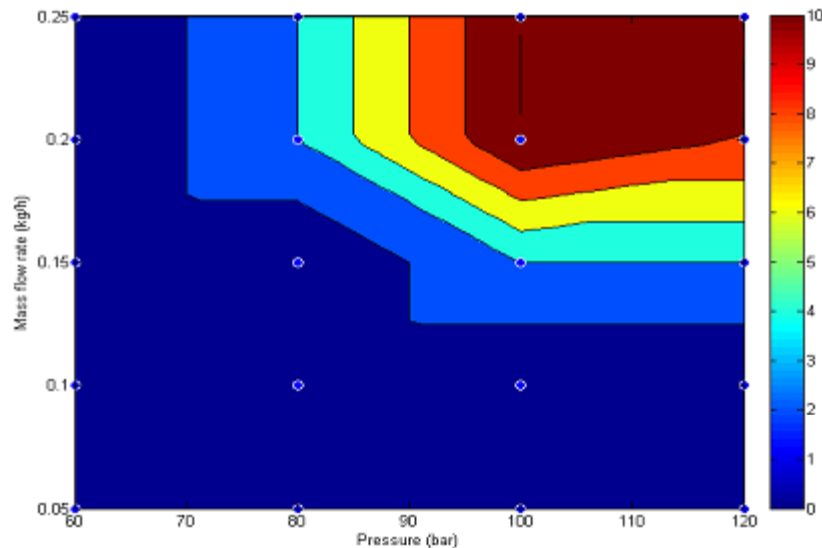


Fig. 7. Liquefaction percentage contours of a small hydrogen liquefier.

Table 6. Convection heat transfer coefficients obtained for different mass flow rates (pressure = 80 bar)

Mass flow rate $\text{kg h}^{-1}$	Convection heat transfer coefficient (inner tube) $\text{J m}^{-2} \text{K}^{-1}$	Convection heat transfer coefficient (annular) $\text{J m}^{-2} \text{K}^{-1}$
0.05	700	49
0.10	1220	85
0.15	1686	117
0.20	2123	148
0.25	2538	177

Table 7. Time and total mass of hydrogen required for producing 1 l liquid hydrogen (pressure =80 bar)

Mass flow rate $\text{kg h}^{-1}$	Time needed for producing 1 l liquid hydrogen (min)	Total mass of hydrogen required (gr)
0.05	No liquid is produced	No liquid is produced
0.10	No liquid is produced	No liquid is produced
0.15	No liquid is produced	No liquid is produced
0.20	12	2400
0.25	9.5	2375

Table 8. Time and total mass of hydrogen required for producing 1 l liquid hydrogen (pressure =100 bar)

Mass flow rate $\text{kg h}^{-1}$	Time needed for producing 1 l liquid hydrogen (min)	Total mass of hydrogen required (gr)
0.05	No liquid is produced	No liquid is produced
0.10	No liquid is produced	No liquid is produced
0.15	10	1500
0.20	5	1000
0.25	4	1000

**Table 9. Time and total mass of hydrogen required for producing 1 l liquid hydrogen (pressure =120 bar)**

Mass flow rate kg h <sup>-1</sup>	Time needed for producing 1 l liquid hydrogen (min)	Total mass of hydrogen required (gr)
0.05	No liquid is produced	No liquid is produced
0.10	No liquid is produced	No liquid is produced
0.15	19	2850
0.20	5.5	1100
0.25	4.5	1125

the pressure leads to a decrease in gas temperature at the expansion valve inlet for lower mass flow rates. Increasing the mass flow rate at a constant pressure leads to a decrease in temperature at the expansion valve inlet. Increasing the pressure has no significant effect on the gas temperature at the expansion valve inlet for high mass flow rates. As a result, using unsuitable values for the mass flow rate and operational pressure might lead to fail liquefaction despite using a heat exchanger with high effectiveness.

## Nomenclature

$A$	Cross section area (m <sup>2</sup> )
$C_p$	Specific heat (J kg <sup>-1</sup> K <sup>-1</sup> )
$D$	Coil diameter (m)
$d$	Tube diameter (m)
$De$	Dean number (dimensionless)
$h$	Convection heat transfer coefficient (W m <sup>-2</sup> K), enthalpy (J kg <sup>-1</sup> )
$k$	Thermal conductivity (W m <sup>-2</sup> K)
$l$	Length (m)
$Nu$	Nusselt number (dimensionless)
$Pr$	Prandtl number (dimensionless)
$P$	Pressure (bar)
$Q_l$	Heat in-leak (W m <sup>-2</sup> )
$r_1$	Internal radius of inner tube (m)
$r_2$	External radius of inner tube (m)
$r_3$	Internal radius of outer tube (m)
$r_4$	External radius of outer tube (m)
$Re$	Reynolds number (dimensionless)
$s$	Entropy (J kg <sup>-1</sup> K <sup>-1</sup> )
$T$	Temperature (K)

$V$	Volume (m <sup>3</sup> )
$z$	Length (m)

## Greek Symbols

$\epsilon$	Emissivity (dimensionless)
$\sigma$	Stefan–Boltzmann constant (W m <sup>-2</sup> K <sup>-4</sup> )
$\rho$	Density (kg m <sup>3</sup> )

## Subscripts

$1$	Warm fluid
$2$	Inner tube wall
$3$	Cold fluid
$4$	Outer tube wall
$a$	Ambient
$c$	Cold surface
$l$	Leakage
$coil$	coil
$ave$	Average

## References

- [1] Garceau N. M., Baik J. H., Lim C. M., Kim S. Y., Oh I.-H., Karng S. W., "Development of a small-scale hydrogen liquefaction system", Int. J. Hydrogen Energy, 2015, 40: 11872.
- [2] Acar C. and Dincer I., "Comparative assessment of hydrogen production methods from renewable and non-renewable sources", Int. J. Hydrogen Energy, 2014, 39: 1.
- [3] Saberimoghaddam A. and Bahri Rasht Abadi M. M.,

"How to Design a Cryogenic Joule-Thomson Cooling System: Case Study of Small Hydrogen Liquefier", *Iranian Journal of Hydrogen & Fuel Cell*, 2016, 3:113.

[4] Saberimoghaddam A., Abadi B. R., Mahdi M., "Evaluation of recuperative tube-in-tube heat exchanger operating in cryogenic refrigeration process: simulation-based transient study", *Asia-Pacific Journal of Chemical Engineering*, 2017, 12: 85.

[5] Damle R. and Atrey M., "The cool-down behaviour of a miniature Joule-Thomson (J-T) cryocooler with distributed J-T effect and finite reservoir capacity", *Cryogenics*, 2015, 71: 47.

[6] Saberimoghaddam A. and Bahri Rasht Abadi M. M., "Influence of tube wall longitudinal heat conduction on temperature measurement of cryogenic gas with low mass flow rates", *Measurement*, 2016, 83: 20.

[7] Pacio J. C. and Dorao C. A., "A review on heat exchanger thermal hydraulic models for cryogenic applications", *Cryogenics*, 2011, 51: 366.

[8] Aminuddin M. and Zubair S. M., "Characterization of various losses in a cryogenic counterflow heat exchanger", *Cryogenics*, 2014, 64: 77.

[9] Krishna V., Spoorthi S., Hegde P. G., Seetharamu K., "Effect of longitudinal wall conduction on the performance of a three-fluid cryogenic heat exchanger with three thermal communications", *Int. J. Heat Mass Transfer*, 2013, 62: 567.

[10] Gupta P. K., Kush P., Tiwari A., "Second law analysis of counter flow cryogenic heat exchangers in presence of ambient heat-in-leak and longitudinal conduction through wall", *Int. J. Heat Mass Transfer*, 2007, 50: 4754.

[11] Nellis G., "A heat exchanger model that includes axial conduction, parasitic heat loads, and property variations", *Cryogenics*, 2003, 43: 523.

[12] Narayanan S. P. and Venkatarathnam G., "Performance of a counterflow heat exchanger with heat loss through the

wall at the cold end", *Cryogenics*, 1999, 39: 43.

[13] Ranganayakulu C., Seetharamu K., Sreevatsan K., "The effects of longitudinal heat conduction in compact plate-fin and tube-fin heat exchangers using a finite element method", *Int. J. Heat Mass Transfer*, 1997, 40: 1261.

[14] Chou F.-C., Pai C.-F., Chien S., Chen J., "Preliminary experimental and numerical study of transient characteristics for a Joule-Thomson cryocooler", *Cryogenics*, 1995, 35: 311.

[15] Tzabar N. and Kaplansky A., "A numerical cool-down analysis for Dewar-detector assemblies cooled with Joule-Thomson cryocoolers", *Int. J. Ref.*, 2014, 44: 56.

[16] Hong Y.-J., Park S.-J., Kim H.-B., Choi Y.-D., "The cool-down characteristics of a miniature Joule-Thomson refrigerator", *Cryogenics*, 2006, 46: 391.

[17] Maytal B., "Cool-down periods similarity for a fast Joule-Thomson cryocooler", *Cryogenics*, 1992, 32: 653.

[18] Chien S. B., Chen L. T., Chou F. C., "A study on the transient characteristics of a self-regulating Joule-Thomson cryocooler", *Cryogenics*, 1996, 36: 979.

[19] Xin R. and Ebadian M., "The effects of Prandtl numbers on local and average convective heat transfer characteristics in helical pipes", *J. Heat Transfer*, 1997, 119: 467.